Numerical Simulation of Smoke Downdrag due to a Sprinkler Spray using FDS

KAI YUAN LI, MICHAEL SPEARPOINT, and CHARLES FLEISCHMANN
Department of Civil and Natural Resources Engineering, University of Canterbury,
Private Bag 4800, Christchurch, 8140, New Zealand

ABSTRACT

Sprinkler interaction with a moving smoke layer, which might lead to smoke downdrag, is numerically simulated by using a large eddy simulation (LES) computational fluid dynamics model, Fire Dynamics Simulator (FDS). The simulations have focused on computing the gas temperature and the smoke layer depth induced by sprinkler discharge into a hot smoke layer. Results are presented for different water flow rates in addition to a simulation of a 'no sprinkler' case. The results of the simulations are compared to measurements from a set of full-scale experiments conducted in previous research and they show that FDS gives fairly good predictions for the upper layer temperature. However FDS underestimates the stability of smoke layer and leads to smoke downdrag regardless of the water flow rate so that the lower region temperatures are higher than those measured in the experiments.

KEYWORDS: sprinkler, interaction, smoke, modelling, CFD, logging, downdrag

NOMENCLATURE LISTING

A_d	surface area of droplet (m^2)	P	operating pressure of the sprinkler (Pa)
C_D	drag coefficient	T_d	temperature of droplet (K)
c	heat capacity of water (J kg^{-1} K^{-1})	T_g	gas temperature (K)
C_{sp}	coefficient for calculating the mean droplet diameter	U	smoke flow velocity (m s^{-1})
d'	diameter of the droplet for integration (m)	U_d	droplet velocity (m s^{-1})
d	diameter of the droplet (m)	We	Weber number
d_m	mean diameter of all droplets (m)	Y_g	water vapor mass fraction at ambient conditions (kg m^{-3})
d_n	diameter of the sprinkler nozzle (m)	Y_d	water vapor mass fraction at saturation conditions (kg m^{-3})
g	acceleration due to gravity (m s^{-2})	**Greek**	
h	convective heat transfer coefficient (W m^{-2} K^{-1})	ρ	density of surrounding air (kg m^{-3})
h_m	mass transfer coefficient (m s^{-1})	ρ_d	density of the water (kg m^{-3})
h_v	heat of evaporation (J kg^{-1})	σ	log-normal distribution coefficient
K	sprinkler flow coefficient (L min^{-1} $bar^{-0.5}$)	γ	Rosin-Rammler distribution exponent
m_d	droplet mass (kg)		

INTRODUCTION

Smoke downdrag, where smoke layer stability is disrupted by a sprinkler spray with the smoke being pulled downwardly, has been investigated by researchers over the past four decades [1 – 6]. In order to describe and then predict the smoke behavior under a sprinkler spray, numerical and especially computational fluid dynamics (CFD) work has been carried out by Chow et al. [7 – 9], Gardiner [10], McGrattan et al. [11] and O'Grady and Novozhilov [12] with different outcomes being obtained by these researchers. By using a

RANS based Euler-Lagrange approach, Chow et al. [7 – 9] developed a CFD model to simulate the interaction between the smoke layer and sprinkler spray. In this model, the water droplets were assumed to be non-evaporating particles which acted as a source term in the smoke momentum and energy equations. The equations were then solved by using the 'Particle-Source-in-Cell' method. The model predictions were compared to the experimental data extracted from the work conducted by Ingason and Olsson [13]. Two parameters, temperature and velocity, were applied in the comparisons. It was found by Chow et al. that the ratio of the lumped drag force generated by all droplets and the buoyancy, which had already been suggested by Bullen [1] to determine the onset of smoke downdrag, was not a commonly suitable approach. In the UK a quasi-field model named SPLASH was developed by Gardiner [10] and later validated by Williams [3]. However as the model was only able to deal with a stable smoke layer, no robust conclusions were made to the feasibility of predicting the smoke downdrag. As Fire Dynamics Simulator (FDS) has become more commonly used, researchers have started to investigate the capability of the model to simulate the smoke layer and sprinkler interaction issue [11, 12]. It is claimed by the researchers that FDS gives reasonably good agreement with experimental data for temperature [11, 12] and the velocity [12]. However it is noted that in the above literature all the experimental validations have been performed outside of the spray region and that the smoke behavior due to the sprinkler spray has not been investigated in any great detail. In order to overcome this limitation, the smoke behavior inside the spray region is studied in this paper with numerical simulations conducted by using FDS. The temperature and the smoke layer shape are compared to previous experimental results so as to validate the FDS simulations.

EXPERIMENTS

Previous experiments [6] have been carried out in an experimental facility as shown in Fig. 1. The experimental set up consisted of two parts; a burning cabin and a sprinkler cabin. The burning cabin was 4 m long, 2 m wide and 2.5 m high. Six air supply intakes each with a 0.8 m by 0.4 m opening were located on both sides of the cabin. Diesel fuelled pool fires were located in the burning cabin to generate an initial smoke layer in the upper region of the sprinkler cabin. The sprinkler cabin was a cube with identical length, width and height dimensions of 4.2 m. A draft curtain with depth of 2.0 m was installed to maintain an initial stable smoke layer thickness of 2.0 m. A 4.2 m high gauge was placed in front of the cabin to measure the depth of the downward smoke plume as shown in Fig. 1(b).

Four thermocouple trees were distributed in a circle of diameter 1.2 m with the sprinkler at the centre. Bare bead K-type thermocouples were used with uncertainties estimated to be of less than ±2 ℃ and the vertical interval of the thermocouples was 0.3 m. The thermocouples were protected by waterproofing caps to avoid the influence of the water droplets on the thermocouple bead. In this study, the temperatures recorded by the downstream thermocouple tree (on the right-hand side of Fig. 1a) were selected to compare with the FDS simulation results. For detailed comparisons, the thermocouples are labeled as TC 1 to TC 13 from the top down to the bottom of cabin.

An open ZSTP-15 Copper Alloys spray sprinkler with a nozzle diameter of 12.7 mm and a flow coefficient of 80 L min^{-1} $bar^{-0.5}$ was used for the experiments. The sprinkler was installed in the centre of the sprinkler cabin roof in a pendant orientation. A pressure reducing valve and pressure transducer were installed in the pipeline to control the sprinkler operating pressure with an accuracy of 0.002 MPa. The sprinkler spray was manually discharged at 50 s after ignition when the upper part of the sprinkler cabin was filled with a stable smoke layer. The operating pressure of sprinkler was varied up to 0.13 MPa. A digital video camera was used to record the experiment so as to determine the length of downdrag smoke (the smoke layer shape) after sprinkler discharge.

Seven experiments which were conducted with an identical heat release rate were selected for the numerical simulations. The heat release rate of the pool fires was determined by the mass loss rate measured by an electronic balance and the calorific value of the diesel which was taken to be 42000 kJ/kg. The total burning time of each test was about 400 s. Previous research obtained the burning efficiency of the diesel as 0.8 and the heat release rates for a free burning 0.8 m by 0.8m pan used in experiments was measured to be 476 kW. The efficiency of the diesel was determined according to previous measurements in an ISO 9705 Calorimeter [14].

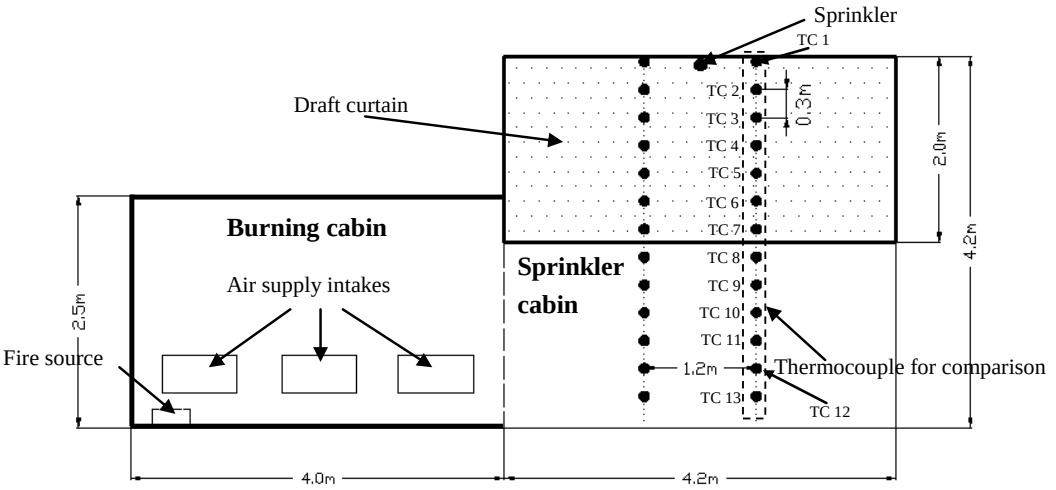

(a) Schematic view

(b) Photo

Fig. 1. Experimental set up (adapted from ref. 6).

FDS MODEL

Water droplets solution

In FDS, the sprinkler spray is modelled by an ensemble of Lagrangian particles with momentum, mass and energy balances for each droplet being governed by [15]

$$\frac{d}{dt}\left(m_d U_d\right) = -\pi \frac{d^2}{8} \rho C_D \left(U_d - U\right)\left|U_d - U\right| - m_d g \qquad (1)$$

$$\frac{dm_d}{dt} = -A_d h_m \left(Y_d - Y_g\right) \qquad (2)$$

$$m_d c \frac{dT_d}{dt} = A_d h \left(T_g - T_d\right) + \frac{dm_d}{dt} h_v \qquad (3)$$

where in Eq. 2, Y_d is the liquid equilibrium vapor mass fraction, which is determined by using the Clausius-Clapeyron equation whereas the local gas phase vapour mass fraction, Y_g, is calculated with the mass

conservation equation for the gas phase. The drag, mass transfer, and energy transfer coefficients are determined by a set of empirical relationships [15].

Not all droplets generated by a sprinkler are numerically computed in FDS but instead sample sets of droplets are released into the computational domain at discrete time steps. The properties of the droplet sample sets are chosen randomly from the pre-specified droplet size distribution. The mass and heat transferred for all droplets are calculated by having the sampled data multiplied by a weighting factor of the total water mass flow. Theoretically, it is inferred that more sampled droplets injected into the computation leads to a higher accuracy. However experiments have only dealt with a set of samples for determining the droplet distributions [16]. The actual number of the droplets generated by a sprinkler is still experimentally uncertain and it is estimated to be 10^5~10^7 particles per second based on the literature [16]. In this study 10^5 particles were generated per second in order to achieve computational efficiency. Further details of the numerical models used in FDS are not discussed here but can be found in the technical reference guide [15].

Model parameters

In order to model a sprinkler spray in FDS, the sprinkler related numerical parameters have to be specified in the input files. Due to the scarcity of detailed descriptions of the spray patterns other than the radius of floor wetting coverage provided by the supplier, the input parameters for the sprinkler used in the experiments had to be reasonably estimated based on various studies reported in the literature.

Sheppard [16] has measured the initial drop sizes and velocities by using particle image velocimetry (PIV) and phase doppler interferometry (PDI) for both pendant and upright sprinklers. For the sprinklers used by Sheppard, the initial droplet velocity was measured to average at 0.6 of $\sqrt{P/\rho_d}$ with an accuracy of 8%. This value was therefore used to specify the sprinkler droplet initial velocity as a model input.

The spray atomisation length, which represents the location at which no further droplet break up occurs downstream from a specific point, was taken as a distance from the sprinkler orifice of 0.2 m based on Sheppard's PIV measurements. This distance correlates well with the estimated value by Novozhilov and co-workers [17, 18].

The droplet volume median diameter, which means half the mass of water is carried by droplets with diameters of d_m or less, was determined by using the equation reported by Yu [19] such that

$$\frac{d_m}{d_n} = C_{sp} We^{-(1/3)} \tag{4}$$

where *We* is the Weber number and C_{sp} is a sprinkler constant. In this case, the value of C_{sp} has been taken to be 1.75 for sprinklers with a 13 mm orifice diameter (15 mm nominal diameter) as obtained by Sheppard [16], which is a more appropriate value in terms of the experimental process to use rather than the 2.33 previously used by Li et al. [6]. Values for C_{sp} vary in the literature, for example Yu [19] gives 2.33 whereas Chow and Cheung [9] suggests 3.2.

The droplet distribution was represented by a combination of log-normal and Rosin-Rammler distributions, which is expressed as:

$$F(d) = \begin{cases} 1 - e^{-0.693\left(\frac{d}{d_m}\right)^{\gamma}} & \left(d > d_m\right) \\ \frac{1}{\sqrt{2\pi}} \int_0^d \frac{1}{\sigma d'} e^{-\frac{\left[\ln(d'/d_m)\right]^2}{2\sigma^2}} dd' & \left(d \le d_m\right) \end{cases} \tag{5}$$

where the empirical coefficients, σ and γ have been previously found to be 0.6 and 2.4 respectively [15].

In terms of Sheppard's work, water discharge occurs along the range of 0~105 ° of the spray angle for the sprinklers with an orifice less than 25 mm. Within this range the maximum water flux occurs between 45~75 ° and the minimum is discharged between 90~105 °. In the simulations studied, the spray angle was

defined to be 0~105 ° in all simulations, which is found to cover the majority of the experiments by Sheppard [16]. As the water flux distribution is not uniform within the range of the spray angle, the actual spray pattern will be slightly different from the simulated one. The spray angle is an issue which might need further investigation. A summary of the input parameters for the sprinkler spray are listed in Table 1.

Table 1. Key input parameters for sprinkler modelling

Key parameters	**Simulation values**
K-factor	80 L min^{-1} $bar^{-0.5}$
Approximate distance from ceiling	0.1 m
Range of operating pressure	0.00 ~ 0.13 MPa
Atomisation length	0.2 m
Droplet volume median diameter	Calculated by Eq. 4 (μm)
Droplet initial velocity	$0.6\sqrt{P/\rho_d}$ (m/s)
Spray angle	0~105 º
Droplets per second	10^5 particles

FDS version 5.2.5 was used for the simulations in this study. Figure 2 shows the computational domain used to represent the experiment and the mesh used. The size of a cube grid was set to 50 mm with up to 1.43 million cells which reached the memory limitation of the available computers. Initial simulations using a coarser mesh with a cell size of 75 mm (identical to that used by O'Grady and Novozhilov [12]) gave similar results to the finer 50 mm grid. The characteristic fire diameter for a 400 kW fire is 0.65 m and therefore a 50 mm mesh was finer than 1/10 of the characteristic fire diameter to meet the requirement for FDS simulations [15]. To reduce overall simulation run times the numerical model was divided into two meshes so as to cover the burning and sprinkler cabins. Comparisons between single mesh and multi mesh simulations on heat release rate and temperature shows that the multi mesh strategy has little influence on the simulation results, as shown in Fig. 3. Two 2.33 GHz processor cores were used in parallel with 2 GB RAM for the numerical calculations on a Windows XP platform.

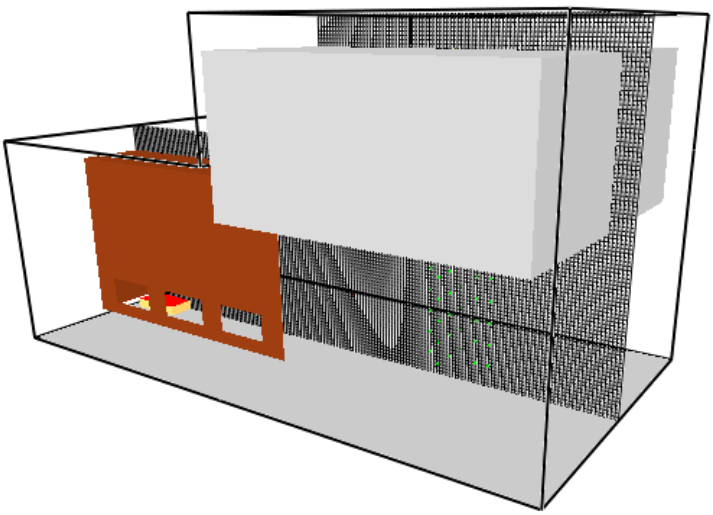

Fig. 2. Computational domain and numerical meshes in FDS.

RESULTS AND DISCUSSION

Smoke temperature predictions

Records of thermocouples TC 1, TC 8 and TC 11 have been selected to be plotted in Fig. 4 where the FDS outputs were given by the "TEMPERATURE" parameter. These particular thermocouples have been chosen as the smoke layer depth was 2 m or slightly more due to the spill plume, the thermocouples

selected therefore respectively represent the top of the smoke layer (TC 1), the interface region between the smoke layer and the fresh air zone (TC 8) and the lower part of the sprinkler cabin (TC 11) which is usually the fresh air zone. The FDS simulation data were outputted at each time step with an interval of 0.3 s and were smoothed using a 50 point averaging and also plotted in Fig. 4.

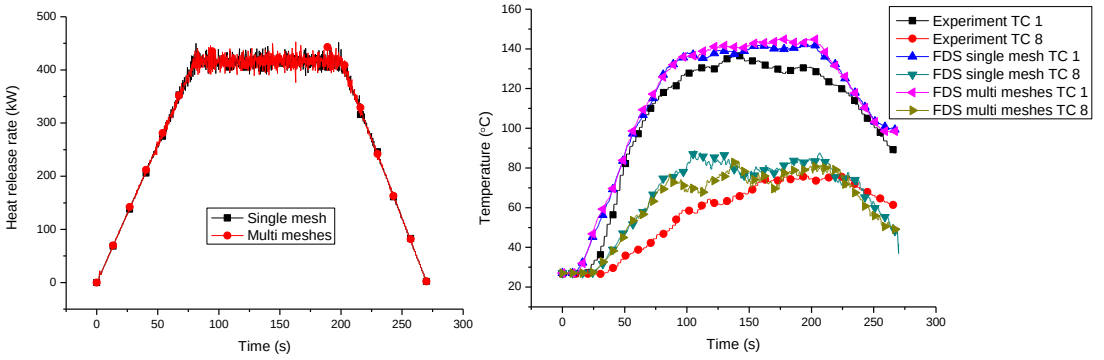

(a) Heat release rate (b) Comparison of TC 1 and TC 8

Fig. 3. Comparison of different mesh setup strategies.

Since the burning cabin was slightly different from the ISO room, the actual heat release rate therefore differed from the measured value. In order to create a similar smoke layer under no sprinkler spray compared to the experiment, the modelled heat release rate was adjusted so that a steady-state peak heat release rate of 420 kW was applied to the numerical simulations. It should be noted that the pool fire needs a certain time to get to the peak heat release rate and decays when the pan began to run out of fuel. In terms of Reference 14, for a 0.8 m square pan, it took about 80 s to reach the peak heat release rate the fire started to decay at 200 s as inferred from the temperature curves. In order to get a similar result which is comparable to the raw data, the fire source in FDS was designated as a gas burner whose heat release rate linearly increases to the peak at 80 s and linearly decays after 200 s until 270 s at which the heat release rate becomes zero.

As shown in Fig. 4(a), the temperatures derived from FDS for the 'no sprinkler' case agree well with the experimental results as would be reasonably expected since the peak steady-state rate of heat release was adjusted to give similar layer conditions to the experiment. Once the sprinkler is operated, it is seen in Fig. 4 that the predictions at the top (TC 1) agree reasonably well with the experimental results. However as to the other thermocouples, the conclusion becomes much less clear. The gap between prediction and experiment expands for the TC 8 cases particularly for the 0.03 MPa and 0.09 MPa experiments. Overall, the predictions for TC 11 give the most scatter in the results. Typically the predicted values are higher than the experimental ones other than the 0.13 MPa experiment where the two curves agree quite well. In terms of the experimental observations, the lower thermocouples were less affected by the steam compared to the upper ones and remained quite dry during the experiments. Therefore the impact of water on the low temperatures measured could be ignored.

In terms of the simulated fire and the temperature curves in the 'no sprinkler' experiment, the period between 100 ~ 200 s could be regarded as a steady state in the experiments. Consequently, the average temperature rise extracted from this time period is plotted as a vertical profile for each case in Fig. 5. The overall impression is that the temperature predictions above the height of 2 m give a relatively good agreement with the experimental records compared to those beneath this height. Typically in the upper region the differences in the temperature rise between the predicted and the experimental values are less than 10 ℃. On the other hand, the difference in the lower region goes up to 30 ℃ (in the 0.03 MPa experiment). In terms of the experimental curves, the temperature difference between the smoke and the air layers are much clearer in the experiments with relatively low operating pressures, so that a robust smoke layer could be defined in these cases. However it is impossible to find a sharp temperature difference which might be used to define a smoke layer in the simulation curves. The lower temperatures predicted are apparently higher than the ambient temperature in all simulations, which partly indicates that the upper smoke originally in the smoke layer before sprinkler operation has been dragged down to the air layer. As a result, the predicted temperatures in the lower region are higher than the experimental values in all cases

studied. These results are contrary to the experiments where it was found that the smoke layer remained stable in cases where the operating pressures were relatively low.

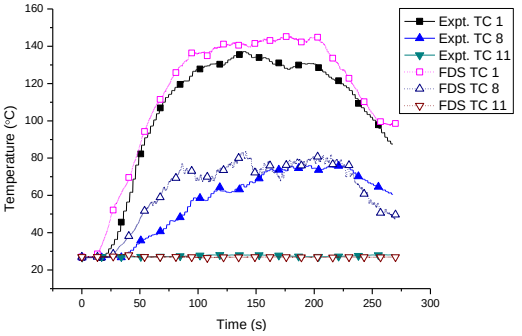

(a) With no sprinkler

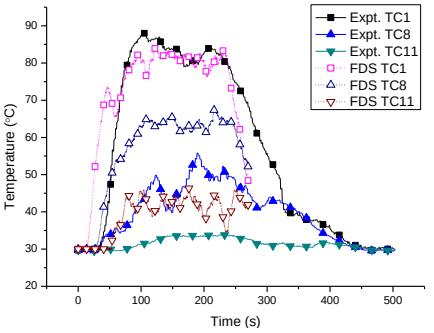

(b) 0.03 MPa

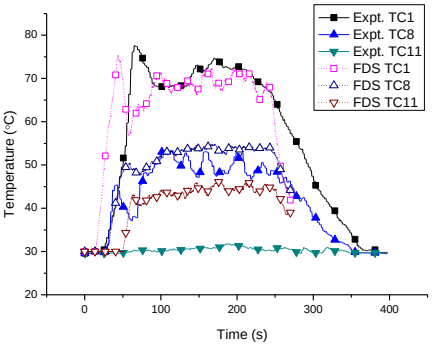

(c) 0.05 MPa

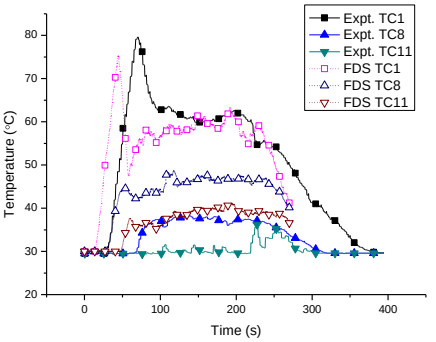

(d) 0.09 MPa

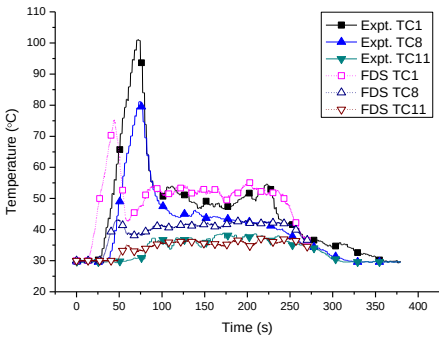

(e) 0.13 MPa

Fig. 4. Temperature curves predicted by FDS at specified sprinkler pressures compared to the experimental recordings.

In order to further investigate the difference between FDS predictions and the experiments, the photographs taken during experiments are compared to the simulation results. In this case, the temperature profiles are used to represent the smoke flow pattern in FDS. The contours are overlaid on the photographs to compare the smoke layer shapes. Comparisons are plotted in Fig. 6 and analysis further confirms that FDS gives a smoke downdrag result regardless of the operating pressure of sprinkler hence the water flow rate. The smoke flow patterns are different between FDS and the experiment. In FDS, the smoke is pulled down to the floor by the sprinkler spray however in the experiment the smoke stops at certain height, which gives a 'bowl' shape of the smoke layer. The most similar case from FDS is the 0.13 MPa experiment where the smoke was dragged almost down to the floor. The temperature comparison also gives a similar result in that the temperature curves are close to each other as shown in Fig. 5(g). Qualitatively, it could therefore be deduced that the predictions from FDS are more accurate as the operating pressure increases.

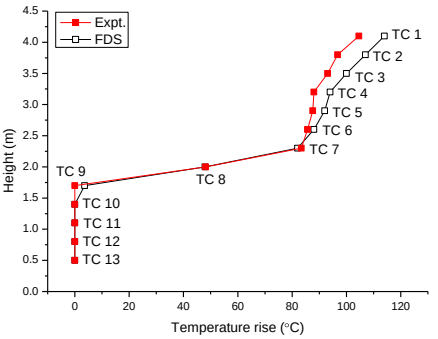

(a) With no sprinkler

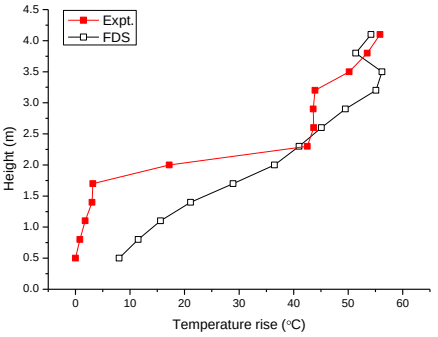

(b) 0.03 MPa

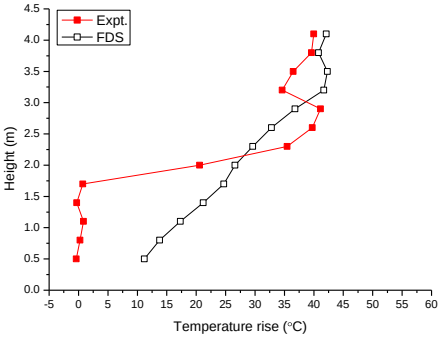

(c) 0.05 MPa

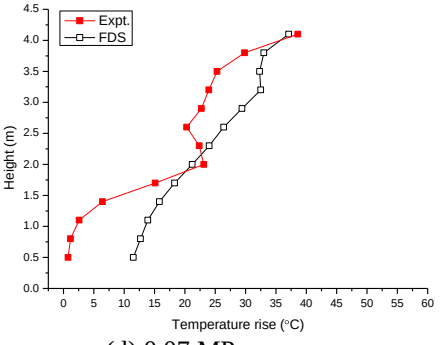

(d) 0.07 MPa

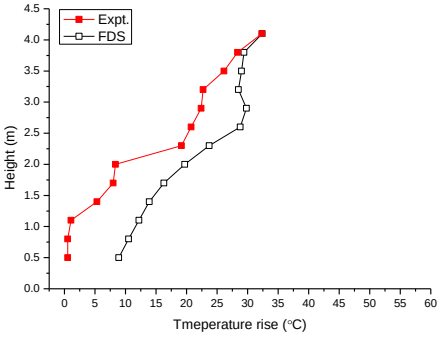

(e) 0.09 MPa

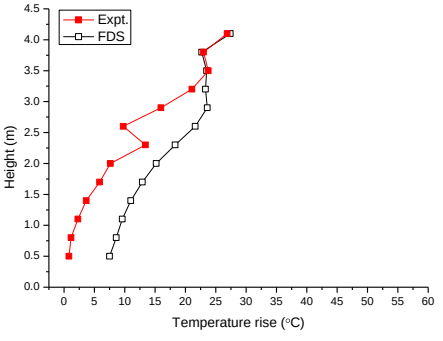

(f) 0.115 MPa

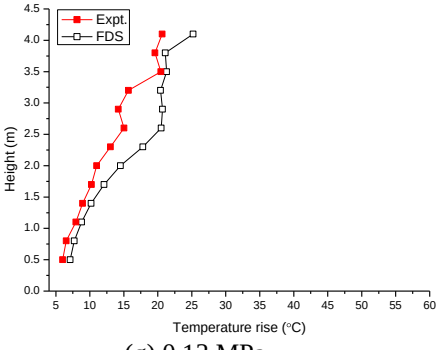

(g) 0.13 MPa

Fig. 5. Comparison between FDS and experimental average temperature rise at steady state.

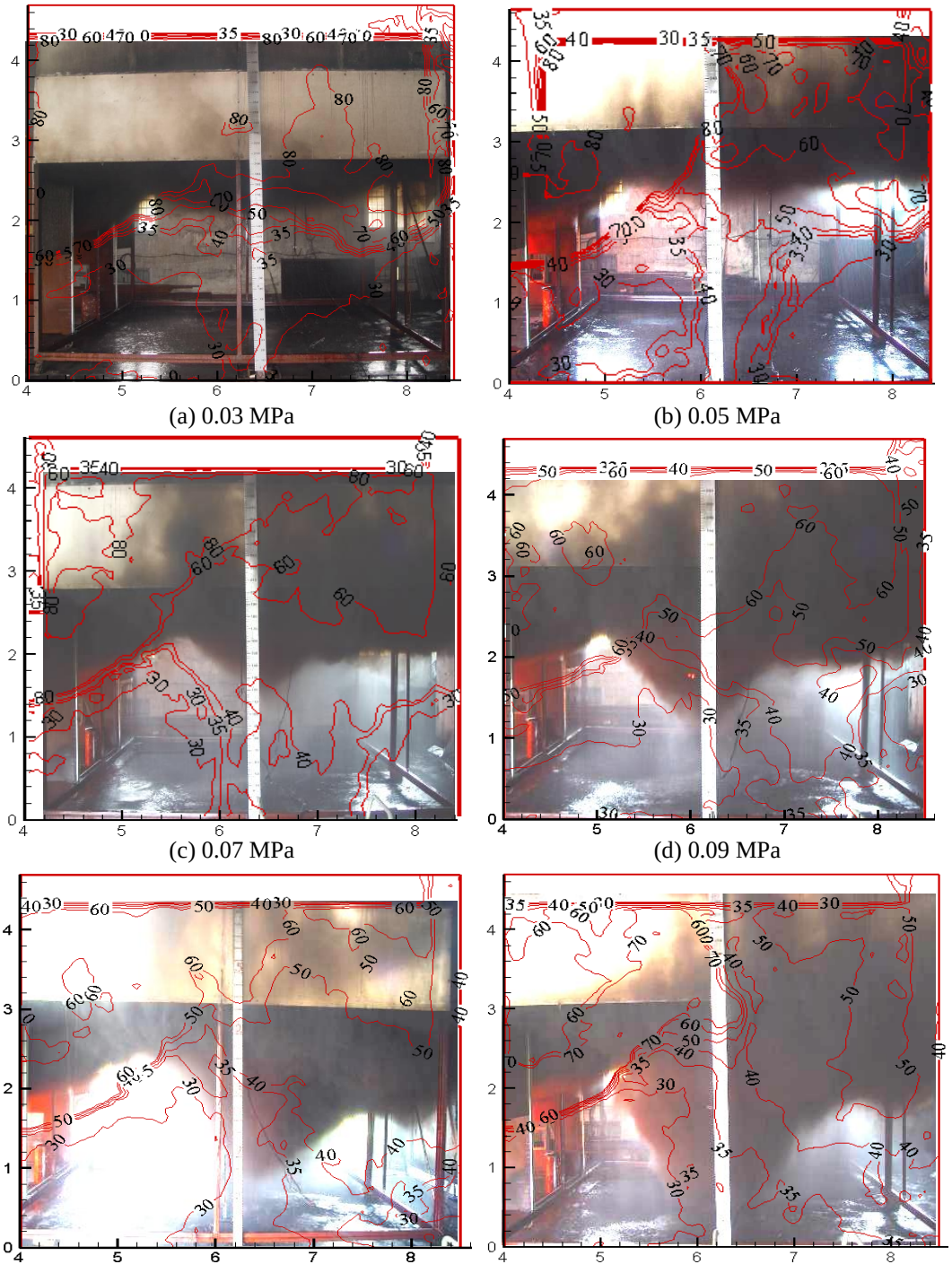

(a) 0.03 MPa (b) 0.05 MPa

(c) 0.07 MPa (d) 0.09 MPa

(e) 0.115 MPa (f) 0.13 MPa

Fig. 6. Comparison between visual smoke observations and FDS temperature contours.

CONCLUSIONS

FDS is applied to numerically model smoke downdrag due to a sprinkler spray. The simulation results are compared to a set of previous experimental data with the temperature and smoke layer shape considered. By appropriately adjusting the peak steady-state rate of heat release it is shown that FDS performs well

with a good agreement for the temperature measurements without sprinkler spray. FDS appears to give a reasonably good prediction of the heat transfer when the sprinkler is discharging. As a result, the temperature predictions above a height of 2 m in the spray region, which is mainly the hot smoke, agree reasonably well with the experiment measurements. However FDS over-predicts the smoke downdrag in the current simulations, which actually leads to smoke being pulled down to the floor regardless of the operating pressure of the sprinkler spray. Therefore the temperatures predicted in the lower part of the spray region are typically higher than the experimental values. The current spray representation assumes the water flux distribution to be uniform over a spray angle of 0~105 °and this might not be the actual spray pattern for the sprinkler. Sensitivity analysis on water flux distribution and spray angle will be carried out later on for further investigation.

ACKNOWLEDGEMENTS

This work was supported by the Opening Fund of State Key Laboratory of Fire Science of University of Science and Technology of China under Grant No. HZ2009-KF01. Kai-Yuan Li is currently the Arup Fire Post-doctorate Fellow at the University of Canterbury. We would also like to acknowledge the New Zealand Fire Service Commission for their support of the Fire Engineering programme at the University of Canterbury.

REFERENCES

[1] Bullen, M.L., (1974) The Effect of a Sprinkler on the Stability of a Smoke Layer Beneath a Ceiling. Fire Research Note 1016, Fire Research Station, Borehamwood, Herts, UK, pp. 1-11.

[2] Heskestad, G., (1991) Sprinkler/hot Layer Interaction, National Institute of Standards and Technology, Technical Report NIST-GCR-91-590, Gaithersburg, MD, USA.

[3] Williams, C., (1993) *The Downward Movement of Smoke due to a Sprinkler Spray*. PhD dissertation, South Bank University, London, UK.

[4] Cooper, L.Y., (1995) The Interaction of an Isolated Sprinkler Spray and a Two-layer Compartment Fire Environment. Phenomena and Model Simulations, Fire Safety Journal, 25: 89–107, http://dx.doi.org/10.1016/0379-7112(95)00037-2

[5] Cooper, L.Y., (1995) The Interaction of an Isolated Sprinkler Spray and a Two-layer Compartment Fire Environment, International Journal of Heat Mass Transfer, 38: 679–690, http://dx.doi.org/10.1016/0017-9310(94)00188-2

[6] Li, K.Y., Hu, L.H., Huo, R., Li, Y.Z., Chen, Z.B., Sun, X.Q. and Li, S.C., (2009) A Mathematical Model on Interaction of Smoke Layer with Sprinkler Spray, Fire safety Journal, 44: 96–105, http://dx.doi.org/10.1016/j.firesaf.2008.04.003

[7] Chow, W.K. and Yao, B., (2001) Numerical Modeling for Interaction of a Water Spray with Smoke Layer, Numerical Heat Transfer, 39: 267-283, http://dx.doi.org/10.1080/104077801300006580

[8] Chow, W.K., and Fong, N.K., (1991) Numerical Simulation on Cooling of the Fire-induced Air Flow by Sprinkler Water Spray, Fire Safety Journal, 17: 263-290, http://dx.doi.org/10.1016/0379-7112(91)90023-R

[9] Chow, W.K. and Cheung, Y.L., (1994) Simulation of Sprinkler-hot Layer Interaction Using a Field Model, Fire and Materials, 18: 359-379, http://dx.doi.org/10.1002/fam.810180604

[10] Gardiner, A.J., *The Mathematical Modelling of the Interaction Between Sprinkler Sprays and the Thermally Buoyant Layers of the Gas from Fires*, PhD dissertation, South Bank Polytechnic, London, United Kingdom, 1989.

[11] McGrattan, K.B., Hamins, A. and Stroup, D., Sprinkler, Smoke & Heat Vent, Draft Curtain Interaction – Large Scale Experiments and Model Development. National Institute of Standards and Technology, Gaithersburg , MD, USA, 1998.

[12] O'Grady, N. and Novozhilov, V., (2009) Large Eddy Simulation of Sprinkler Interaction with a Fire Ceiling Jet, Combustion Science and Technology, 181: 984-1006, http://dx.doi.org/10.1080/00102200902973158

[13] Ingason, H. and Olsson, S., Interaction Between Sprinklers and Fire Vents, SP Report 1992.11, Sweden Swedish National Testing and Research Institute, 1992.

[14] Yi, L., *Study on Smoke Movement and Management in Atrium Building*. PhD dissertation, University of Science and Technology of China, Hefei, Anhui, China, 2005.

[15] McGrattan, K., *Fire Dynamics Simulator Technical Reference Guide*, version 5, NIST special publication 1018, 2004.

[16] Sheppard, D.T., *Spray Characteristics of Fire Sprinklers*. PhD dissertation, Northwestern University, Evanston, USA, 2002.

[17] Novozhilov, V., Harvie, D.J.E., Green, A.R. and Kent, J.H., (1997) A Computational Fluid Dynamic Model of Fire Burning Rate and Extinction by Water Sprinkler, Combustion Science and Technology, 123: 227-245, http://dx.doi.org/10.1080/00102209708935629

[18] Novozhilov, V., Harvie, D.J.E., Kent, J.H., Apte, V.B. and Pearson, D., (1997) A Computational Fluid Dynamics Study of Wood Fire Extinguishment by Water Sprinkler, Fire Safety Journal, 29: 259-282, http://dx.doi.org/10.1016/S0379-7112(97)00027-1

[19] Yu, H.Z., Investigation of Spray Patterns of Selected Sprinklers with the FMRC Drop Size Measuring System, *Fire Safety Science – Proceedings of the First International Symposium*, International Association for Fire Safety Science, 1986, pp. 1165–1176, http://dx.doi.org/10.3801/IAFSS.FSS.1-1165